Structural Basis of Substrate Recognition in Thiopurine *S*-Methyltransferase[†,‡]

Yi Peng,[§] Qiping Feng,[||] Dennis Wilk,[§] Araba A. Adjei,[||,⊥] Oreste E. Salavaggione,[||,⊥] Richard M. Weinshilboum,[||] and Vivien C. Yee*[,§]

Department of Biochemistry, Case Western Reserve University, Cleveland, Ohio 44106, and Department of Molecular Pharmacology and Experimental Therapeutics, Mayo Clinic College of Medicine—Mayo Clinic, Rochester, Minnesota 55905

Received January 18, 2008; Revised Manuscript Received April 16, 2008

ABSTRACT: Thiopurine *S*-methyltransferase (TPMT) modulates the cytotoxic effects of thiopurine prodrugs such as 6-mercaptopurine by methylating them in a reaction using *S*-adenosyl-L-methionine as the donor. Patients with TPMT variant allozymes exhibit diminished levels of protein and/or enzyme activity and are at risk for thiopurine drug-induced toxicity. We have determined two crystal structures of murine TPMT, as a binary complex with the product *S*-adenosyl-L-homocysteine and as a ternary complex with *S*-adenosyl-L-homocysteine and the substrate 6-mercaptopurine, to 1.8 and 2.0 Å resolution, respectively. Comparison of the structures reveals that an active site loop becomes ordered upon 6-mercaptopurine binding. The positions of the two ligands are consistent with the expected S_N2 reaction mechanism. Arg147 and Arg221, the only polar amino acids near 6-mercaptopurine, are highlighted as possible participants in substrate deprotonation. To probe whether these residues are important for catalysis, point mutants were prepared in the human enzyme. Substitution of Arg152 (Arg147 in murine TPMT) with glutamic acid decreases V_{max} and increases K_m for 6-mercaptopurine but not K_m for *S*-adenosyl-L-methionine. Substitution at this position with alanine or histidine and similar substitutions of Arg226 (Arg221 in murine TPMT) result in no effect on enzyme activity. The double mutant Arg152Ala/Arg226Ala exhibits a decreased V_{max} and increased K_m for 6-mercaptopurine. These observations suggest that either Arg152 or Arg226 may participate in some fashion in the TPMT reaction, with one residue compensating when the other is altered, and that Arg152 may interact with substrate more directly than Arg226, consistent with observations in the murine TPMT crystal structure.

Thiopurines such as 6-mercaptopurine (6MP),[1] 6-thioguanine, and azothioprine are cytotoxic and are immunosuppressant compounds which are used to treat childhood acute lymphoblastic leukemia, inflammatory bowel disease, and transplant rejection (*1–3*). They are prodrugs which are extensively metabolized to give thioguanine nucleotides that exert their cytotoxic effects by incorporation into DNA or inhibiting purine synthesis. Thiopurine *S*-methyltransferase (TPMT) is a cytosolic enzyme which modulates the cytotoxicity of thiopurines by taking them as substrates in an S-methylation reaction. TPMT is a classic example of pharmacogenetics, in which allelic variation in patients results in a range of drug response (*4, 5*). Variant alleles result in TPMT enzymes whose activities range from barely detectable to near wild-type level, and as a consequence a 10−15-fold range in thiopurine dosage is necessary in order to minimize toxicity and other complications in patients.

The TPMT reaction takes two substrates, the methyl donor *S*-adenosyl-L-methionine (AdoMet) and a methyl acceptor, and generates *S*-adenosyl-L-homocysteine (AdoHcy) and a methylated product. Although 6-MP and other thiopurines are well characterized as TPMT methyl acceptors, a natural substrate for this enzyme has yet to be identified. The crystal structure of human TPMT bound to AdoHcy and the NMR structure of a bacterial TPMT orthologue have been reported (*6, 7*). While these structures characterized the TPMT fold and the AdoMet binding site, they did not reveal the details of methyl acceptor recognition. We report here the crystal structures of murine TPMT bound to AdoHcy, with and without 6-MP additionally present in the methyl acceptor binding site. These structures demonstrate structural and conformational features of 6-MP binding and highlight

[†] This work was supported by National Institutes of Health Grant U01 GM61388, The Pharmacogenetics Research Network (Y.P., D.W., A.A.A., V.C.Y., R.M.W.). V.C.Y. is an Established Investigator of the American Heart Association. Use of the Argonne National Laboratory Structural Biology Center beamlines at the Advanced Photon Source was supported by the U.S. Department of Energy, Office of Biological and Environmental Research, under Contract No. W-31-109-ENG-38. The Advanced Light Source is supported by the Director, Office of Science, Office of Basic Energy Sciences, of the U.S. Department of Energy under Contract No. DE-AC02-05CH11231.

[‡] Coordinates and structure factors for mTPMTwt-AdoHcy and mTPMTwt-AdoHcy-6MP have been deposited in the Protein Data Bank with accession codes 3BGI and 3BGD, respectively.

* To whom correspondence should be addressed: phone, (216) 368-1184; fax, (216) 368-3419; e-mail, vivien.yee@case.edu.

[§] Case Western Reserve University.

[||] Mayo Clinic College of Medicine—Mayo Clinic.

[⊥] Current address: Roswell Park Cancer Institute.

[1] Abbreviations: TPMT, thiopurine *S*-methyltransferase; mTPMT, murine TPMT; hTPMT, human TPMT; AdoMet, *S*-adenosyl-L-methionine; AdoHcy, *S*-adenosyl-L-homocysteine; 6MP, 6-mercaptopurine; MAD, multiple wavelength anomalous dispersion; SAMT, salicylic acid carboxyl methyltransferase; PrmC, N^5-glutamine methyltransferase, the product of the protein release factor methylation gene; PAPT, putrescine aminopropyltransferase; TIMP, thioinosine monophosphate; dcAdoMet, decarboxylated *S*-adenosyl-L-methionine; AdoDATO, *S*-adenosyl-1,8-diamino-3-thiooctane.

10.1021/bi800102x CCC: $40.75
Published on Web 05/17/2008

two nearby arginine residues which were subsequently tested by mutagenesis for their role in substrate binding and TPMT activity.

MATERIALS AND METHODS

Protein Expression and Purification. The full-length mTPMT and hTPMT coding regions were amplified by PCR from eukaryotic expression plasmids (*8*) and cloned into the *Nde*I and *Eco*RI sites of pET-28a (Novagen) to give expression constructs coding for TPMTs with an N-terminally fused His_6 tag. Transformed *Escherichia coli* BL21(DE3) cells were grown at 37 °C to an OD_{600} of ~0.8 before induction with 0.4 mM IPTG and were incubated for an additional 8 h at 37 °C. Cells were then harvested by centrifugation and resuspended in lysis buffer (50 mM Tris-HCl, pH 7.9, 500 mM NaCl, and 5 mM imidazole) with the protease inhibitor cocktail set II (Calbiochem) for sonication. After centrifugation, the supernatant was loaded onto Ni^{2+}-NTA resin (Qiagen) and washed with the lysis buffer, and the expressed TPMT protein was eluted with 50 mM Tris-HCl, pH 7.9, 500 mM NaCl, and 150 mM imidazole. The pooled eluted fractions were dialyzed against 50 mM Tris-HCl, pH 8.2, and 2 mM DTT. Final purification was by gel filtration on a Superdex 75 column 10/300 GL (Amersham Biosciences) equilibrated with 20 mM Tris-HCl, pH 8.0. MALDI-MS analysis of the purified mTPMT revealed that both AdoMet and AdoHcy had copurified with mTPMT, with AdoHcy the major species of the two (data not shown; Mass Spectrometry Facility, Institute of Pathology, Case Western Reserve University). Selenomethionine- (SeMet-) substituted mTPMT was obtained with the same expression system by inhibition of methionine biosynthesis (*9*) and purified as above except that 5 mM DTT was added in dialysis and gel filtration. Point mutations in the hTPMT expression plasmid were prepared using the QuikChange site-directed mutagenesis kit (Stratagene), and the hTPMT mutants were expressed and purified using the wild-type protocol.

Enzyme Activity Assays. TPMT enzyme activity was measured with a radiochemical assay based on the methylation of 6MP with [*methyl*-^{14}C]AdoMet as the methyl donor (*10*). The reaction mixture contained 7.5 mM 6MP (Sigma), 24.2 μM AdoMet (7.2 μCi/μmol; Perkin-Elmer), 1 mM DTT, 50 μM allopurinol, and 150 mM KH_2PO_4 buffer (pH 6.5). For substrate kinetic experiments, 6MP concentrations varied from 30 μM to 7.5 mM and AdoMet concentrations ranged from 0.09 to 48.4 μM. One unit of TPMT activity represented the formation of 1 nmol of 6-methylmercaptopurine per second of incubation at 37 °C. The kinetic experiments were carried out in triplicate, and standard deviations were calculated for the average values of K_m and V_{max} determined (Table 2).

Crystallization and Data Collection. All crystals were grown by sitting drop vapor diffusion at 20 °C using a protein concentration of ~6 mg/mL and a 1:1 protein: precipitant volume ratio. Four different mTPMT crystal forms were grown from a variety of conditions which fell into four types: condition 1 with 22−32% (w/v) PEG3350, 0.2 M lithium sulfate/ammonium sulfate, and 0.1 M imidazole/Mes/bis-tris, pH 5.2−6.5; condition 2 with 20−22% PEG3350 and 0.15 M malic acid (pH 5.5); condition 3 with 30−35% pentaerythritol ethoxylate, 0.05 M ammonium sulfate, and 0.05 M imidazole/Mes/bis-tris (pH 6.0−6.5); and condition 4 with 20% PEG3350 and 0.2 M potassium sulfate. Crystals of mTPMTwtSeMet-AdoHcy were grown from condition 1 with 25−32% (w/v) PEG3350 and 0.1 M imidazole (pH 5.2−6.0). mTPMTwt complex crystals were grown by mixing proteins with AdoHcy (2 mM), AdoMet (5 mM), and 6MP (10 mM), respectively. Crystals of mTPMTwt-AdoHcy-6MP were grown from condition 1 with 25−27% (w/v) PEG3350 and 0.1 M imidazole (pH 5.5) and from condition 2. Crystals of mTPMTwt-AdoMet were obtained from condition 1 with 22−27% (w/v) PEG3350 and 0.1 M imidazole/Mes (pH 6.0 or 6.5) and from conditions 2 and 3. mTPMTwt-AdoHcy crystals grew from condition 4. Crystals were cryoprotected in artificial mother liquor containing 35% (w/v) PEG3350 or pentaerythritol ethoxylate and flash cooled in liquid nitrogen. All data were collected at APS beamlines 19ID (mTPMTwt-AdoHcy-6MP, mTPMTwt-AdoHcy,) and 19BM (SeMet-mTPMT-AdoHcy). The data were processed with HKL (*11*) (Table 1). Crystals belong to space group $P2_1$ and contain two molecules in each asymmetric unit.

Structure Determination and Refinement. SeMet MAD data were measured at the peak and edge wavelengths (0.97877 and 0.97888 Å) at APS 19BM from a mTPMTwt-SeMet-AdoHcy crystal. Initial heavy atom sites were found with SOLVE (*12*) and improved by RESOLVE (*13, 14*), such that the mean figure of merit increased from 0.29 to 0.59. During the model-building process, an unpublished structure of truncated hTPMT with AdoHcy was deposited in the Protein Data Bank (PDB accession code 2BZG) and was used to aid the interpretation of electron density maps. The initial mTPMTwt-AdoHcy model was in turn used to solve the mTPMTwt-AdoHcy-6MP structures. Interactive model building was carried out with COOT (*15*), and refinement calculations were performed in CNS (*16*) and REFMAC (*17*). The quality of all models was assessed by PROCHECK (*18*). The majority of the residues are located in the most favored region of the Ramachandran plot. No clear electron density for the N-terminal His_6 tag and 8−9 residues of mTPMT was observed, and these residues were not included in the final models. A summary of the final refinement statistics is provided in Table 1. Molecular figures were generated using PyMol (*19*).

RESULTS

Overall Structures of TPMT Complexes. Crystallization experiments of all possible binary and ternary complexes of mTPMTwt with AdoMet, AdoHcy, and 6MP were carried out, and crystals were grown in the presence of AdoMet, AdoHcy, and AdoHcy with 6MP. The electron density maps revealed that AdoHcy was bound in all crystal forms, even in those which were grown from mTPMT incubated with AdoMet, presumably due to the predominance of AdoHcy which copurified with mTPMT. The many crystal forms grown thus resulted in two unique crystal structures of two different complexes: mTPMTwt-AdoHcy and mTPMTwt-AdoHcy-6MP (Table 1). These structures both confirmed that mTPMTwt possesses the expected class I AdoMet-dependent MTase core fold (*20–22*), which consists of a seven-stranded β sheet flanked on each side by three α helices (Figure 1A).

Table 1: Data Collection, Phasing, and Refinement Statistics[a]

	SeMet-wt-AdoHcy			
	peak	inflection	wt-AdoHcy	wt-AdoHcy-6MP
Data Collection				
cell dimensions				
a, *b*, *c* (Å)	62.60, 66.09, 72.86	62.57, 66.12, 72.92	62.91, 65.51, 72.90	62.89, 69.78, 72.23
β (deg)	115.48	115.53	115.29	115.78
wavelength (Å)	0.97877	0.9788	1.0332	0.97912
resolution (Å)[a]	50−2.5 (2.59−2.5)	50−2.5 (2.59−2.5)	50−1.8 (1.86−1.8)	30−2.0 (2.07−2.0)
R_{sym}	12.6 (38.2)	13.4 (43.2)	4.6 (34.1)	7.3 (26.3)
$I/\sigma I$	10.8 (3.8)	9.7 (2.5)	31.4 (4.7)	13.0 (3.5)
completeness (%)	99.4 (99.1)	99.1 (95.7)	98.5 (96.6)	96.9 (83.6)
redundancy	4.1 (3.9)	3.9 (3.1)	4.9 (4.9)	2.9 (2.4)
Refinement				
resolution (Å)			50−1.8 (1.86−1.8)	30−2.0 (2.07−2.0)
no. of reflections			46591	35011
R_{work}/R_{free}			18.74 (22.07)	20.89 (26.21)
no. of atoms: protein, ligand, water			3746, 52, 456	3760, 92, 307
average *B* factors: protein, AdoHcy, 6MP, water			25.8, 17.3, −, 30.9	24.3, 14.7, 40.9, 29.6
rmsd[b]				
bond lengths (Å)			0.013	0.013
bond angles (deg)			1.440	1.461
Ramachandran				
most favored (%)			89.1	92.8
additionally allowed (%)			10.7	7.2
disallowed (%)			0.2	0.0

[a] Numbers in parentheses refer to the highest resolution shell. [b] rmsd, root-mean-square deviation.

Table 2: Enzyme Activity of TPMT Wild-Type and Mutant Proteins

		AdoMet		6MP	
mTPMT	hTPMT	K_m (μM)	V_{max} (units/mg of protein)	K_m (mM)	V_{max} (units/mg of protein)
wt		5.6 ± 0.5	0.96 ± 0.05	0.350 ± 0.014	0.604 ± 0.016
	wt	18.5 ± 1.7	1.59 ± 0.16	0.68 ± 0.17	1.23 ± 0.03
	Arg152Ala	25.4 ± 1.4	1.18 ± 0.06	2.73 ± 0.23	1.49 ± 0.07
	Arg152Glu	44.5 ± 3.6	**0.32** ± 0.05	**4.63** ± 1.75	**0.51** ± 0.16
	Arg152His	23.7 ± 2.2	1.25 ± 0.10	1.43 ± 0.39	0.92 ± 0.17
	Arg226Ala	19.7 ± 2.4	1.24 ± 0.14	1.61 ± 0.11	1.59 ± 0.04
	Arg226Glu	14.8 ± 1.4	1.16 ± 0.05	1.2 ± 0.15	1.37 ± 0.06
	Arg226His	19.9 ± 2.2	1.55 ± 0.09	0.91 ± 0.13	1.26 ± 0.06
	Arg152Ala/Arg226Ala	46.3 ± 12.5	**0.50** ± 0.13	**6.32** ± 0.37	**0.426** ± 0.014

The mTPMT structure has several modifications to the MTase core: an additional 40 residues at the N-terminus, a reversed β hairpin inserted from residues Tyr102−Ser122, and a small helix (Glu220−Trp225) inserted between the last two β strands. A DALI structural database search with the mTPMT coordinates identified over 50 similarly folded proteins, all with <20% shared sequence identity (*23*), but limited information on acceptor substrate binding. Only five structural matches are of complexes with both the methyl donor and acceptor binding sites occupied. Of these, the two most similar structural homologues are phenylethanolamine *N*-methyltransferase (*24*) (3.1 Å rmsd for 189 superimposed Cα atoms, 12% sequence identity) and histamine *N*-methyltransferase (*25*) (3.6 Å rmsd for 178 superimposed Cα atoms, 12% sequence identity), each bound to AdoHcy and an inhibitor. Both ternary complexes revealed inhibitors bound in positions or orientations too far away from the AdoHcy (>7 Å) to represent productive acceptor substrate binding modes. The remaining three complex structures reveal ligands bound productively in the acceptor binding site and are of *Clarkia breweri* salicylic acid carboxyl methyltransferase (SAMT, 3.4 Å rmsd for 191 superimposed Cα atoms, 8% sequence identity) (*26*), *Thermotoga maritima* N^5-glutamine methyltransferase (product of the protein release factor methylation gene, PrmC, 3.2 Å rmsd for 155 superimposed Cα atoms, 10% sequence identity) (*27*), and *T. maritima* putrescine aminopropyltransferase (PAPT, 3.5 Å rmsd for 166 superimposed Cα atoms, 7% sequence identity) (*28*).

For each complex crystal structure, there are two copies of mTPMT in the asymmetric unit. Superpositions of the Cα atoms for molecules in the same crystal and across crystals give overall rmsd of 0.2−0.8 and 0.8−1.0 Å, respectively. Unless otherwise stated, structural details provided in the following sections are for the mTPMTwt-AdoHcy-6MP structure and are similar in the mTPMTwt-AdoHcy complex.

AdoHcy Binding to TPMT. The electron density for AdoHcy is well-defined in both mTPMT molecules in both structures and clearly shows that AdoHcy is present since there is no density corresponding to the sulfur-bound methyl group characteristic of AdoMet (Figure 1B). As seen in other class I MTases, AdoHcy binds to mTPMT in an extended conformation at the N-terminal half of the central β sheet, with the N-terminal extension and inserted helix covering the occupied active site (Figure 1A,B). Hydrogen-bonding interactions between AdoHcy and mTPMT are similar to those in other class I MTase structures (*24, 29*). The AdoHcy terminal amine group forms hydrogen bonds with a water molecule and the carbonyl oxygen atoms of Leu64 and

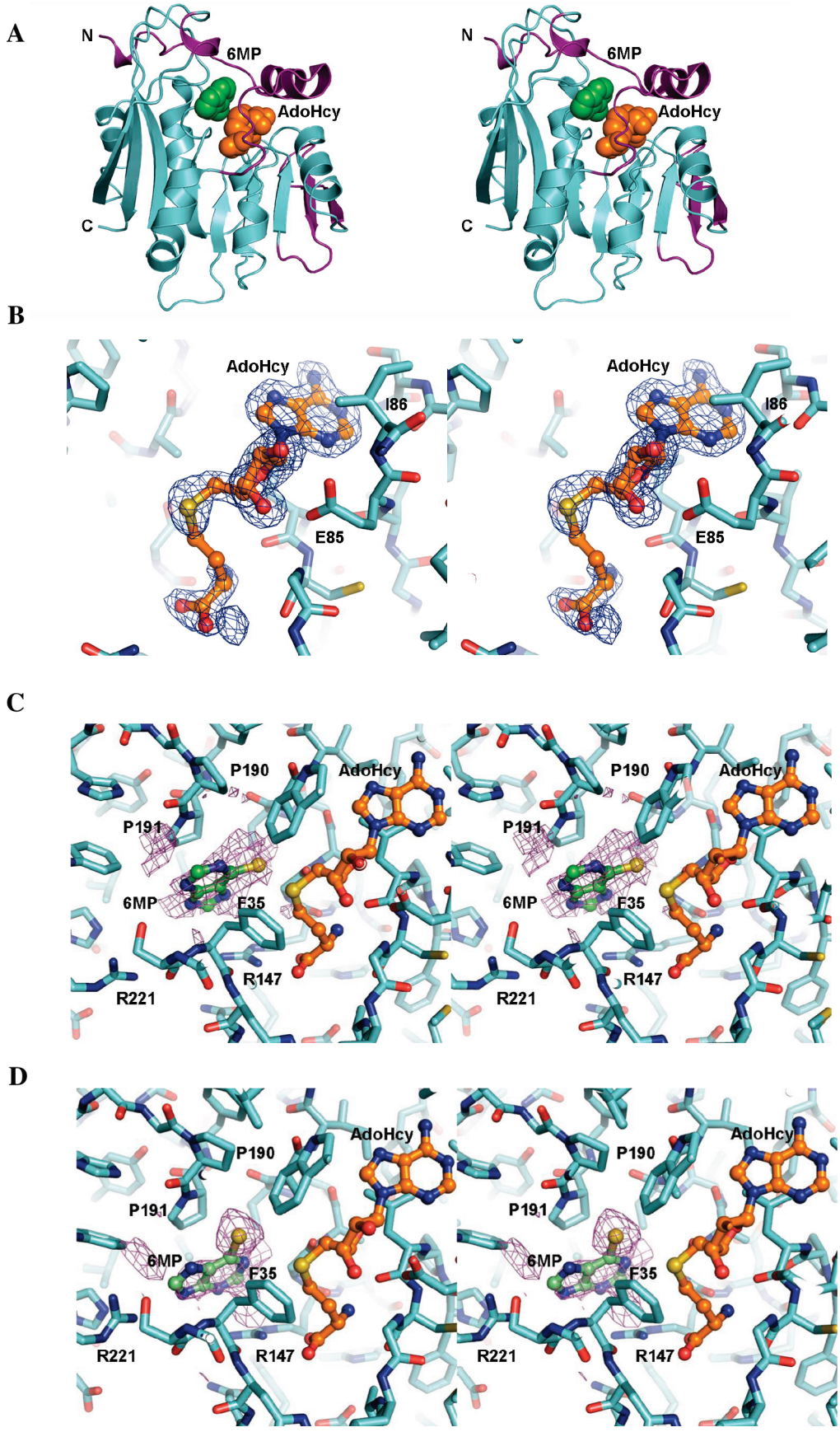

FIGURE 1: Crystal structures of mTPMT. (A) Stereo ribbon diagram of mTPMT. The conserved class I MTase core is shown in cyan, and the inserted regions characteristic of the TPMT structure are in purple. AdoHcy (orange) and 6MP (green) are shown as space-filling spheres. (B) AdoHcy bound to the active site of molecule A in mTPMTwt-AdoHcy. Stereoview of 1.8 Å resolution omit $|F_o| - |F_c|$ density contoured at 3σ is shown; similar density is present for molecule B and for the two AdoHcy molecules in mTPMTwt-AdoHcy-6MP. (C) 6MP bound to the active site of mTPMTwt-AdoHcy-6MP. Stereoview of 2.0 Å resolution omit $|F_o| - |F_c|$ density contoured at 1.5σ is shown for the 6MP bound to molecule A. (D) Similar omit density for 6MP bound to molecule B.

Arg147 in all four complex molecules. The ligand's carboxylate is surrounded by a more flexible region of the protein and participates in different sets of interactions in different structures, interacting with one or two solvent molecules as well as with the side chain of Arg147 (only in mTPMTwt-AdoHcy-6MP). The AdoHcy ribose hydroxyl groups form hydrogen bonds with the Trp28 and Glu85 side chains while the adenine's ring nitrogen atoms interact with the main chain amines of Ile86 and Ile130 and a water molecule. Among the other contacts that stabilize AdoHcy binding is the sandwiching of the adenine ring between the Leu64 and Ile86 side chains. AdoHcy binding to mTPMTwt, when comparing the two molecules within each crystal and between the two crystal structures, is with the ligand in essentially the same position in identical conformations (rmsd of ~0.4 Å for pairwise superpositions). Of the AdoHcy binding residues (Figure 2A,B), those whose side chains interact with AdoHcy (Trp28, Leu64, Glu85, Ile86) are conserved in not only human and murine but also other mammalian TPMTs (Figure 3); Ile130, which is involved in only a main chain interaction, is conservatively substituted with a leucine in some of the other mammalian sequences.

6MP Binding to TPMT. Class I MTases bind AdoMet (or the demethylated product AdoHcy) at the same methyl donor site in their structures, reflecting their shared AdoMet dependence, but must have diverse active sites to accommodate their wide variety of acceptor substrates (*20*). In the mTPMT complex structures, the electron density for the 6MP acceptor substrate is weaker and less defined than for AdoHcy (Figure 1C,D), which is consistent with the observation that the 6MP binding affinity is weaker than that of AdoMet by 2−3 orders of magnitude (Table 2). For one molecule in the mTPMTwt-AdoHcy-6MP, the electron density had a flattened shape suitable for the bicyclic purine structure, but the location of the protruding thiol was ambiguous (Figure 1C). The 6MP was modeled in each of the two possible positions, related by ~180° rotation perpendicular to the plane of the rings. Upon each possible 6MP position was superimposed the structure of thioinosine monophosphate (TIMP), a larger TPMT substrate which is an intermediate in thiopurine metabolism (*30*). TIMP was found to fit in only one orientation without severe clashes with the TPMT polypeptide backbone. This orientation was chosen for final refinement of 6MP since the two TPMT substrates are expected to bind similarly in the active site due to their high degree of chemical similarity. The density for the second molecule in mTPMTwt-AdoHcy-6MP was defined enough to allow identification of the sulfur position and thus of the 6MP orientation (Figure 1D).

The mTPMTwt-AdoHcy-6MP structure shows the 6MP bound to the two independent molecules similarly, in essentially the same position in the active site but in different orientations (Figures 2C,D and 4A). The intersulfur distances of 3.4 and 4.1 Å for the two molecules are about double the 1.85 Å length of a sulfur−carbon single bond, consistent with the presumption that AdoMet-dependent MTases adopt a conserved S_N2-like mechanism in which the methyl group is transferred directly from AdoMet to the acceptor (*27*). Participating in no direct hydrogen-bonding interactions with the protein, 6MP is bound in the active site by a number of van der Waals interactions (Figure 2A,B). Pro191 and Pro190 are conserved in all TPMTs (Figure 3), and their *cis*-peptide bonds define one face of the 6MP binding site. In addition, the side chains of Pro191 and Phe35, conserved in all mammalian TPMTs, form a hydrophobic clamp that orients the 6MP purine ring. Arg147, which forms a salt bridge with the AdoHcy carboxylate, and Arg221 are the only hydrophilic residues within 4 Å of 6MP and thus are the only candidates that may possibly be involved in the deprotonation of 6MP which is expected before the subsequent methylation by AdoMet. Arg147 is about 3 Å from 6MP in both mTPMT-AdoHcy-6MP complexes, while Arg221 is 3.2 and 5.4 Å from 6MP in the two molecules.

A Flexible Active Site Loop in TPMT. Structural comparisons of the two molecules in each of the mTPMTwt-AdoMet and mTPMTwt-AdoHcy-6MP structures highlight regions which change conformation upon 6MP binding. The two molecules in mTPMTwt-AdoHcy superimpose to give an rmsd of 0.8 Å for all Cα atoms. The regions whose conformations differ the most between the two molecules are residues Ser34−His47, which form an extended loop over the active site (the "active site loop", Figure 2C,D), and residues Glu220−Trp225, which is a short helix in an adjacent loop that contains Arg221, one of the two arginine residues which is near the bound 6MP in mTPMTwt-AdoHcy-6MP. It is interesting to note that these two segments are not part of the core protein fold of the class I AdoMet-dependent MTases and are characteristic of TPMT structure. When these regions are omitted from the superposition, the Cα rmsd drops to 0.2 Å. These two regions also have a much higher average *B* factor (70 $Å^2$) than for the rest of the molecule (21 $Å^2$), characteristic of high flexibility. In contrast, the two molecules in mTPMTwt-AdoHcy-6MP superimpose to give a low 0.2 Å rmsd for all Cα atoms, and the average *B* factor for the two loop regions (36 $Å^2$) is much closer to that of the rest of the protein (23 $Å^2$), suggesting that upon 6MP binding the active site loop and the adjacent Arg221-containing helix become ordered. A similar superposition of the mTPMTwt-AdoHcy and mTPMTwt-AdoHcy-6MP structures highlights the extended active site loop (Arg31−Gln55) and nearby Glu220−Trp225 helix as the segments which change the most upon 6MP binding: the pairwise Cα rmsd values drop from 0.8−1.0 to 0.3−0.5 Å when the two regions are omitted.

Structure-Based Mutagenesis of TPMT. To investigate whether either of the arginine residues near the bound 6MP is important for enzyme activity, single and double mutants were prepared in the more biomedically relevant hTPMT. In the single mutants, Arg152 in hTPMT (Arg147 in mTPMT) or Arg226 (Arg221 in mTPMT) was substituted with either alanine, glutamic acid, or histidine. The double mutant hTPMT Arg152Ala/Arg226Ala was also generated. Enzyme activity assays were carried out using radiolabeled AdoMet, and substrate kinetic experiments were performed by varying AdoMet and 6MP concentrations separately (Table 2). Most of the mutants exhibit K_m and V_{max} values which are similar to those of the wild-type enzyme. The only mutants which deviate substantially from wild-type activity are Arg152Glu and Arg152Ala/Arg226Ala. When Arg152 is replaced with an oppositely charged glutamic acid, the K_m for the 6MP acceptor, but not for the AdoMet donor, increases significantly (by ~7-fold), and the V_{max} decreases modestly by ~2−5-fold.

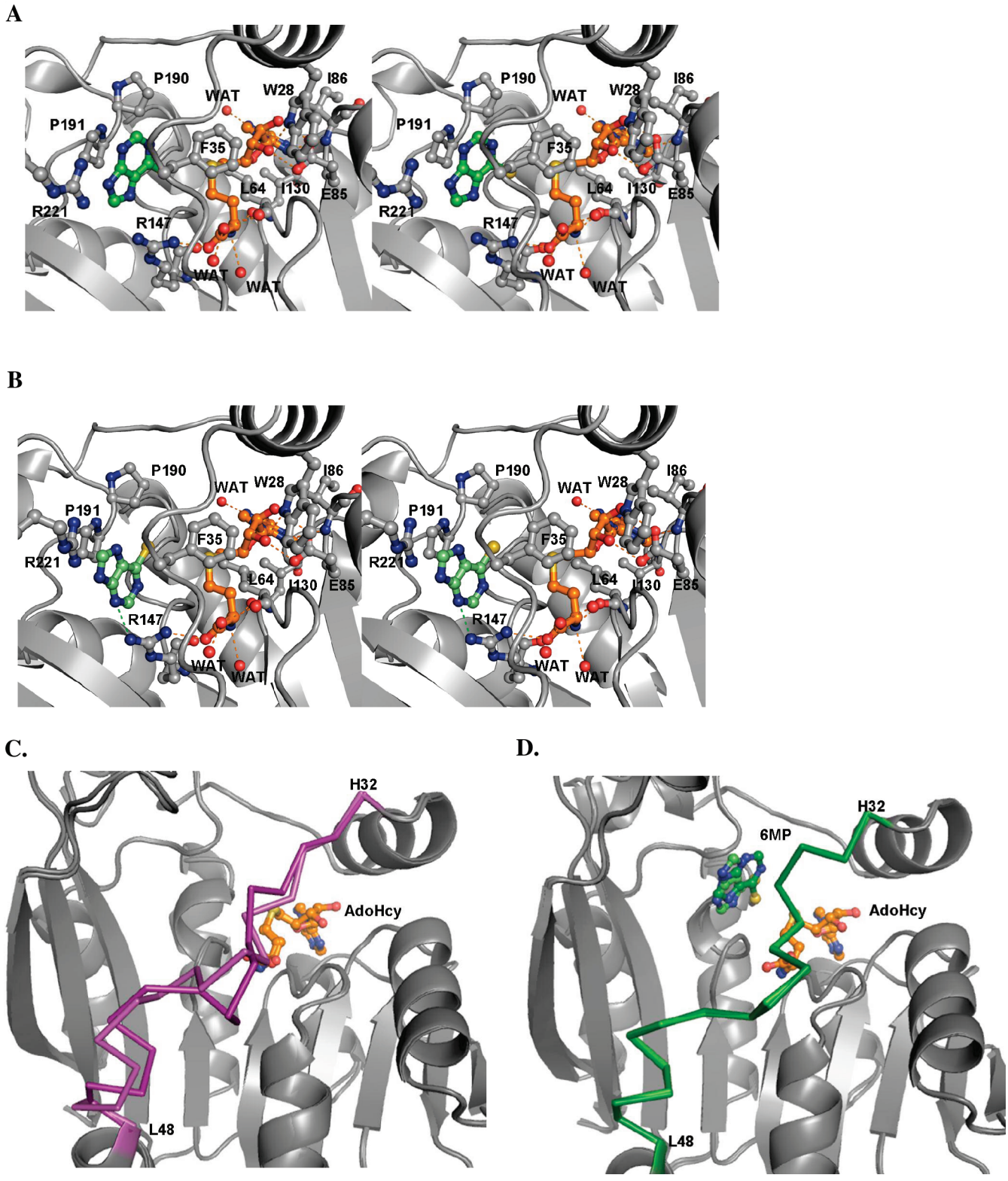

FIGURE 2: Ligand binding to mTPMT. (A, B) Stereoviews of the active sites of molecules A and B in the mTPMTwt-AdoHcy-6MP structure. AdoHcy, 6MP, and side chains of nearby mTPMT residues are shown as ball-and-stick structures. (C) Active site loop flexibility in mTPMTwt-AdoHcy. Superposition of molecules A and B shows that the active site loop (purple) is flexible and adopts two different conformations. (D) Active site loop conformation in mTPMTwt-AdoHcy-6MP. When both AdoHcy and 6MP are bound, the superimposed active site loops (green) become better ordered and adopt the same conformation.

Similarly, when both arginine residues are substituted with alanines, a small decrease in V_{max} (~3-fold) accompanies a substantial increase in K_m for 6MP (~9-fold) while the K_m for AdoMet is not significantly altered.

DISCUSSION

While TPMT's ability to methylate thiopurine prodrug substrates is well characterized, natural substrates for this

```
mTPMT      -----MSLDMKEHPDAEVQKNQVLTLEDWKEKWVTRHISFHQEQGHQLLKKHLDTFLKGQSGLRVFFPLCGKAIE 70
hTPMT      MDGTRTSLDIEEYSDTEVQKNQVLTLEEWQDKWVNGKTAFHQEQGHQLLKKHLDTFLKGKSGLRVFFPLCGKAVE 75
gTPMT      MDGTRTSLDIEEYSDTEVQKNQVLTLEEWQDKWVNGKTAFHQEQGHQLLKKHLDTFLKGKSGLRVFFPLCGKAVE 75
chTPMT     MDGTRTSLDIEEYSDTEVQKNQVLTLEEWQDKWVNGKTAFHQEQGHQLLKKHLDTFLKGKSGLRVFFPLCGKAVE 75
dTPMT      MDKTRTFLDVKEYPDTEVQKNRVLTLEEWQEKWVSRRIGFHQEQGHKLLKKHLDTFLKGENGLRVFFPLCGKAVE 75
cTPMT      MDDTSTLIDVKEYPDTEVQKNRVLTLEEWREKWVDGKIGFHQEQGHQLLKKHLDTFLKGENVLRVFFPLCGKAVE 75
psTPMT     -------------------------------------GSHQSEVNKDLQQYWSSLN-VVPGARVLVPLCGKSQD 36

mTPMT      MKWFADRGHTVVGVEISEIGIREFFAEQNLSYTEEPLAEIAGAKVFKSSSGSISLYCCSIFDLPRANIGKFDRIW 145
hTPMT      MKWFADRGHSVVGVEISELGIQEFFTEQNLSYSEEPITEIPGTKVFKSSSGNISLYCCSIFDLPRTNIGKFDMIW 150
gTPMT      MKWFADRGHSVVGVEISELGIQEFFTEQNLSYSEEPITEIPGTKVFKSSSGNISLYCCSIFDLPRTNIGKFDMIW 150
chTPMT     MKWFADRGHSVVGVEISELGIREFFTEQNLSYSEEPITEIPGTKVFKSSSGNISLYCCSIFDLPRTNIGKFDMIW 150
dTPMT      MKWFADRGHSVVGVEISELGIREFFAEQNLSYTEEPIVEIPGGKIFKSSSGNISLYCCSLFDLPRANIGKFDRIW 150
cTPMT      MKWFADRGHCVVGVEISELGIREFFTEQNLSYSEEPIMEIPGAKVFKSSSGNISLYCCNLFDLPRVNIGKFDRIW 150
psTPMT     MSWLSGQGYHVVGAELSEAAVERYFTER----GEQPHITSQGDFKVYAAPG-IEIWCGDFFALTARDIGHCAAFY 106

mTPMT      DRGALVAINPGDHDRYADIILSLLRKEFQYLVAVLSYDPTKHAGPPFYVPSAELKRLFGTKCSMQCLEEVDALEE 220
hTPMT      DRGALVAINPGDRKCYADTMFSLLGKKFQYLLCVLSYDPTKHPGPPFYVPHAEIERLFGKICNIRCLEKVDAFEE 225
gTPMT      DRGALVAINPGDRKCYADTMLSLLGKKFQYLLCVLSYDPTKHPGPPFYVPHAEIERLFGKICNIRCLEKVDAFEE 225
chTPMT     DRGALVAINPGDRKCYADTMLSLLGKKFQYLLCVLSYDPTKHPGPPFYVPHAEIERLFGKICNIRCLEKVDAFEE 225
dTPMT      DRGALVAINPGDRERYADIMLSLTRKGFHYLLAVLCYDPTKHAGPPFYVPEAEIKKLFGSICNIHCLEKVDVFEE 225
cTPMT      DRGALVAVNPGDRKCYTDIMLSLTRKGFRYLLAVLSYDPTKHPGPPFYVPDAEIKNLFGSTCNIHCLEKVDVFEE 225
psTPMT     DRAAMIALPADMRERYVQHLEALMPQACSGLLITLEYDQALLEGPPFSVPQTWLHRVMSGNWEVTKVGGQDTLHS 181

mTPMT      RHK--AWGLDYLFEKLYLLTEK 240
hTPMT      RHK--SWGIDCLFEKLYLLTEK 245
gTPMT      RHK--SWGIDCLFEKLYLLTEK 245
chTPMT     RHK--SWGIDCLFEKLYLLTEK 245
dTPMT      QHK--SWGIDYIIEKLYLFTEK 245
cTPMT      RHK--SWGIDYIVEKLYLLTEK 245
psTPMT     SARGLKAGLERMDEHVYVLERV 203
```

FIGURE 3: Alignment of TPMT and related sequences. Sequences of six representative mammalian TPMTs and one bacterial TPMT are included (NCBI accession numbers): mouse (mTPMT, AAC25919), human (hTPMT, AAB27277), gorilla (gTPMT, AAX37643), chimpanzee (chTPMT, AAX37639), dog (dTPMT, AAL18006), cat (cTPMT, Q6EIC1), and *Pseudomonas syringae* (psTPMT, PDB 1pjz). Residues involved in AdoHcy binding (orange), 6MP binding (green), and hTPMT polymorphisms (blue) are highlighted.

enzyme have yet to be identified. To obtain some structural understanding of TPMT substrate recognition, the crystal structures of mTPMT with and without its 6MP acceptor substrate bound were determined. Consistent with the 80% sequence conservation, the mTPMT protein fold is very similar to that of hTPMT, for which cocrystallization efforts with acceptor substrate were unsuccessful (*7*), and to an unpublished crystal structure of mTPMT deposited in the PDB during the course of this work that also did not contain bound acceptor substrate (accession code 2GB4). The rmsd for equivalent Cα atoms when the mTPMT-AdoHcy and mTPMT-AdoHcy-6MP crystal structures are superimposed with that of hTPMT-AdoHcy (*7*) are 1.1 and 0.7 Å, respectively, and AdoHcy is bound in the same conformation in the active sites of the two enzymes. Both mTPMTwt and hTPMTwt have higher affinity for AdoMet (low micromolar) than for 6MP (low millimolar) (Table 2). This difference is consistent with the larger accessible surface area buried and greater number of ligand−protein hydrogen bonds formed upon AdoHcy binding to mTPMTwt (~400 Å^2, 6−7 hydrogen bonds) compared to 6MP binding to the enzyme (~200 Å^2, 1 hydrogen bond). Reflecting its modest binding affinity, 6MP interacts with the enzyme through hydrophobic and van der Waals interactions, in a relatively loose manner reflected by its two different orientations in the two independent molecules in the mTPMTwt-AdoHcy-6MP crystal structure (Figure 2A,B).

A structural database search identified crystal structures of SAMT (*26*), PrmC (*27*), and PAPT (*28*) as the most similar ternary complexes for comparison with TPMT. Of these enzymes, TPMT, SAMT, and PrmC use AdoMet as a methyl donor while PAPT uses decarboxylated AdoMet (dcAdoMet) as an aminopropyl donor; all four enzymes bind their donor substrates in similar positions and orientations (Figure 4). Class I MTases are expected to bind donor and acceptor molecules in a manner consistent with an S_N2-like reaction mechanism involving direct transfer between substrates (*27, 31*), and their active sites are expected to be chemically and structurally diverse to accommodate a variety of acceptor substrates (*20*). The mTPMTwt-AdoHcy-6MP structure reveals 6MP-AdoHcy sulfur−sulfur distances of 3.4−4.1 Å, consistent with direct methyl transfer (Figure 4A). Superposition of the mTPMT ligands with the AdoHcy and salicylic acid in the SAMT active site (salicylic acid−AdoHcy oxygen−sulfur distances of 4.3−4.7 Å) and the AdoMet and N^5-methylglutamine bound to PrmC (glutamine−AdoMet nitrogen−sulfur distances of 3.3−3.8 Å) show that the acceptor molecules are bound in similar positions and orientations relative to their corresponding donor molecule

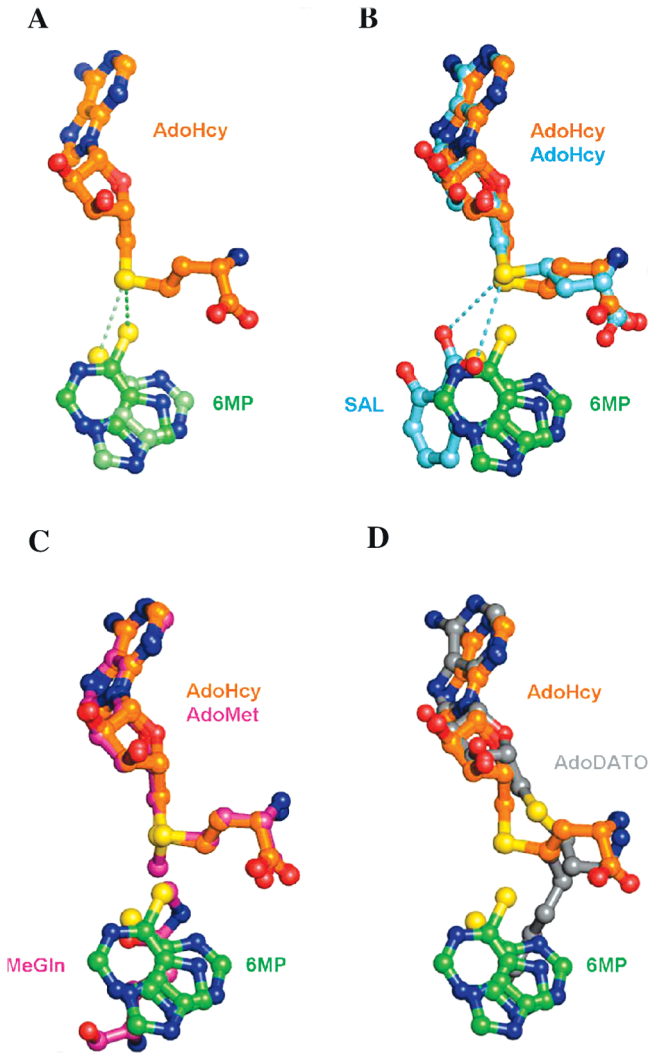

FIGURE 4: Donor and acceptor substrate binding to MTase fold enzymes. (A) AdoHcy demethylated donor and 6MP acceptor bound to mTPMTwt-AdoHcy-6MP. Superposition of the AdoHcy bound to molecules A and B shows that the two 6MP are in the same position but different orientations. Dashed lines represent the possible path of methyl transfer between the AdoHcy and 6MP sulfur atoms. (B) AdoHcy demethylated donor and salicylic acid acceptor bound to SAMT (*26*). Superposition of the SAMT and mTPMT structures shows that salicylic acid and 6MP approach their respective AdoHcy from the same general direction. Dashed lines represent possible paths of methyl transfer between the salicylate carboxylate oxygen atoms and the AdoHcy sulfur in SAMT. (C) AdoMet donor and N^5-methylglutamine methylated acceptor bound to PrmC (*27*). Both methylated PrmC ligands represent mixtures of (de)methylated donor (AdoMet and AdoHcy) and acceptor (methylglutamine and glutamine) molecules. Superposition of the PrmC and mTPMT structures shows that N^5-methylglutamine and 6MP approach their respective AdoMet/AdoHcy in similar fashion. (D) The bisubstrate adduct inhibitor AdoDATO bound to PAPT (*28*). The adenosyl and aminopropyl groups at opposite ends of AdoDATA superimpose well with the adenosyl group of AdoHcy and 6MP bound to mTPMT. The central region of AdoDATA is in a different conformation from the homocysteine moiety of AdoHcy, probably reflecting the differences in the aminopropyl and methyl groups transferred and in the (de)carboxylated states of the donor molecules.

(Figure 4B,C). The similar juxtaposition of donor and acceptor molecules is striking considering that these three enzymes transfer methyl groups to different types of atoms (sulfur, oxygen, and nitrogen), in chemically diverse acceptor substrates. The bisubstrate adduct inhibitor *S*-adenosyl-1,8-diamino-3-thiooctane (AdoDATO) bound to the aminopropyltransferase PAPT identifies donor and acceptor binding sites which coincide with those of the three methyltransferases, although the conformation of the dcAdoMet donor moiety of the inhibitor differs from that seen for AdoHcy/AdoMet in the methyltransferase structures, reflecting the absence of the carboxylate group in the donor, the different chemical group transferred, and the covalent attachment of donor and acceptor substrate groups (Figure 4D).

The MTase reaction mechanism also requires a deprotonation step before, during, or after the methyl transfer (*27*). Inspection of the hTPMT-AdoHcy crystal structure led to speculation that Lys32 and Arg226 may be candidates for substrate deprotonation (*7*). The mTPMTwt-AdoHcy-6MP structure presented here provides a first view of acceptor substrate bound to the TPMT active site. The closest approach of mTPMT Lys27 (homologous to hTPMT Lys32) to 6MP is ~6−7 Å, too long for this residue to participate in substrate deprotonation. Superposition of the human and mouse structures shows that hTPMT Lys32 and mTPMT Lys27 are in very similar conformations and that Lys32 is also ~6 Å from 6MP. Only two hydrophilic residues are found within 4 Å of the 6MP bound in the mTPMT active site: Arg147 and Arg221 (Arg152 and Arg226 in hTPMT). Arg147 in both molecules in the mTPMT structure and Arg152 in the hTPMT structure are in nearly identical positions and conformations, and all are about 3 Å from 6MP (for Arg152, when the hTPMT and mTPMT structures are superimposed). In contrast, the mTPMT Arg221 and hTPMT Arg226 conformations are less conserved, and the closest approaches to 6MP are 3.0 and 5.3 Å (two molecules in mTPMT) and 2.7 and 3.5 Å (hTPMT superimposed onto the two mTPMT molecules). Substitution of either Arg152 or Arg226 residues in hTPMT with alanine, glutamic acid, or histidine resulted in modestly diminished enzyme activity for only Arg152Glu (Table 2). Tandem mutations of both residues gave Arg152Ala/Arg226Ala, which also exhibited modestly compromised activity. The average decreases in V_{max} are ~3-fold for both Arg152Glu and Arg152Ala/Arg226Ala, while K_m increased 7- and 9-fold for the single and double mutants, respectively. These observations are consistent with the proximity of the two arginine residues to the 6MP acceptor and suggest that these two residues, while not essential for TPMT activity, nonetheless may play a role in the reaction by contributing to 6MP binding. That the double alanine mutant has altered V_{max} and K_m for 6MP when the single alanine substitutions have wild-type behavior suggests that the two arginines have overlapping roles such that one residue may compensate when the other is altered. That the only single mutant with altered behavior is Arg152Glu indicates that this residue may contribute more than Arg226, consistent with the more direct interaction of the homologous Arg147 with 6MP that is observed in the mTPMTwt-AdoHcy-6MP structure. The greater importance of Arg152 is also consistent with this residue (mTPMT Arg147) being conserved among all TPMTs while Arg226 (mTPMT Arg221) can vary (Figure 3). The modest effect on V_{max} for these designed TPMT mutants suggests that neither arginine is responsible for substrate deprotonation. In addition, the mTPMT ternary structure does not highlight any solvent molecule or other moiety near the bound 6MP

that can be speculated to prepare the 6MP thiol group for the methyltransferase reaction by general acid/base catalysis. The absence of a general base or solvent molecule near the acceptor substrate in mTPMT is a shared observation with the SAMT and PrmC ternary complexes; for the latter the deprotonation step is speculated to occur during or following product release (*27*).

Comparison of the mTPMTwt-AdoHcy and mTPMTwt-AdoHcy-6MP structures reveals that a loop containing residues Arg31−Gln55 that extends over the active site and an adjacent helical turn (Glu220−Trp225) which includes Arg221 are the two regions which change conformation most upon 6MP binding. The active site loop is very flexible in the absence of 6MP, as evidenced by weak density, high *B* factors, and high rmsd between the two mTPMT molecules (Figure 2C,D); upon 6MP binding, this segment is characterized by well-defined density, lower *B* factors which are similar to those for the rest of the protein, and a low rmsd between the two molecules. This pronounced conformational alteration of the mTPMT active site loop is reminiscent of a 10-residue "gatekeeping" loop in PAPT which changes conformation and becomes ordered upon AdoDATA binding. Interestingly, the PAPT loop corresponds to mTPMT residues Arg147−Gly156; while this loop does not change conformation in mTPMT upon 6MP binding, it contains the Arg147 which interacts with the acceptor substrate. Acceptor substrate diffusion through a solvent channel to the active site has been proposed upon surface analysis of the hTPMT crystal structure without acceptor ligand bound (*7*). The characterization of a flexible active site loop in mTPMT identifies an alternative or additional structural feature which plays a role in substrate access and recognition.

The two mTPMT crystal structures reported here identify molecular features that are important for the enzyme's catalytic function. The structures reveal an active site which binds 6MP in two different, overlapping orientations. Other TPMT substrates in thiopurine metabolism include 6-thioguanine and the nucleotides 6-thioinosine 5′-monophosphate and 6-thioguanosine 5′-monophosphate (*30*), which result from coupling of thiopurines to phosphoribosylpyrophosphate by hypoxanthine phosphoribosyltransferase. Structural modeling confirms that these larger acceptor substrates can be accommodated in both bound 6MP orientations since the phosphoribosyl groups would be directed away from the binding site toward solvent. The other and more effective known TPMT acceptor substrates are thiophenol derivatives (*32, 33*); their K_m values of 2−3 orders of magnitude less than that of 6MP illustrate that the presence of a heterocyclic aromatic ring is not necessary for substrate recognition, consistent with the observation of few hydrophilic residues near the bound 6MP. Although natural TPMT substrates have yet to be identified, the flexibility and partial solvent accessibility of the 6MP binding site suggest that TPMT may be capable of binding molecules which are substantially larger than 6MP and the related thiopurine metabolites. In addition to aiding speculation on the nature of natural TPMT substrates, the structural features of the acceptor binding site might also be exploited in designing small molecule modulators or customizing drugs which may allow optimization of thiopurine-based therapy.

ACKNOWLEDGMENT

We thank S. Ginell and J. Nix for beamline support and F. van den Akker for helpful discussions.

REFERENCES

1. Paterson, A. R. P., and Tidd, D. M. (1975) *6-Thiopurines*, Springer-Verlag, New York.
2. Lennard, L. (1992) The clinical pharmacology of 6-mercaptopurine. *Eur. J. Clin. Pharmacol. 43*, 329–339.
3. Coulthard, S., and Hogarth, L. (2005) The thiopurines: an update. *Invest. New Drugs 23*, 523–532.
4. Cheok, M. H., and Evans, W. E. (2006) Acute lymphoblastic leukaemia: a model for the pharmacogenomics of cancer therapy. *Nat. Rev.Cancer 6*, 117–129.
5. Wang, L., and Weinshilboum, R. (2006) Thiopurine S-methyltransferase pharmacogenetics: insights, challenges and future directions. *Oncogene 25*, 1629–1638.
6. Scheuermann, T. H., Lolis, E., and Hodsdon, M. E. (2003) Tertiary structure of thiopurine methyltransferase from *Pseudomonas syringae*, a bacterial orthologue of a polymorphic, drug-metabolizing enzyme. *J. Mol. Biol. 333*, 573–585.
7. Wu, H., Horton, J. R., Battaile, K., Allali-Hassani, A., Martin, F., Zeng, H., Loppnau, P., Vedadi, M., Bochkarev, A., Plotnikov, A. N., and Cheng, X. (2007) Structural basis of allele variation of human thiopurine-S-methyltransferase. *Proteins: Struct., Funct., Bioinf. 67*, 198–208.
8. Salavaggione, O. E., Wang, L., Wiepert, M., Yee, V. C., and Weinshilboum, R. M. (2005) Thiopurine S-methyltransferase pharmacogenetics: variant allele functional and comparative genomics. *Pharmacogenet. Genomics 15*, 801–815.
9. van Duyne, G. D., Standaert, R. F., Karplus, P. A., Schreiber, S. L., and Clardy, J. (1993) Atomic structures of the human immunophilin FKBP-12 complexes with FK506 and rapamy. *J. Mol. Biol. 229*, 105–124.
10. Weinshilboum, R. M., Raymond, F. A., and Pazmino, P. A. (1978) Human erythrocyte thiopurine methyltransferase: radiochemical microassay and biochemical properties. *Clin. Chim. Acta 85*, 323–333.
11. Otwinowski, Z., and Minor, W. (1997) Processing of x-ray diffraction data collected in oscillation mode. *Methods Enzymol. 276*, 307–325.
12. Terwilliger, T. C., and Berendzen, J. (1999) Automated MAD and MIR structure solution. *Acta Crystallogr. D 55*, 849–861.
13. Terwilliger, T. C. (2000) Maximum-likelihood density modification. *Acta Crystallogr. D 56*, 965–972.
14. Terwilliger, T. C. (2003) Automated main-chain model building by template matching and iterative fragment extension. *Acta Crystallogr. D 59*, 38–44.
15. Emsley, P., and Cowtan, K. (2004) Coot: model-building tools for molecular graphics. *Acta Crystallogr. D 60*, 2126–2132.
16. Brunger, A. T., Adams, P. D., Clore, G. M., DeLano, W. L., Gros, P., Grosse-Kunstleve, R. W., Jiang, J. S., Kuszewski, J., Nilges, M., Pannu, N. S., Read, R. J., Rice, L. M., Simonson, T., and Warren, G. L. (1998) Crystallography & NMR system: A new software suite for macromolecular structure determination. *Acta Crystallogr. D 54*, 905–921.
17. Murshudov, G. N., Vagin, A. A., and Dodson, E. J. (1997) Refinement of macromolecular structures by the maximum-likelihood method. *Acta Crystallogr. D 53*, 240–255.
18. Laskowski, R. A., MacArthur, M. W., Moss, D. S., and Thornton, J. M. (1993) PROCHECK: a program to check the stereochemical quality of protein structures. *J. Appl. Crystallogr. 26*, 283–291.
19. DeLano, W. L. (2004)The PyMOL Molecular Graphics System, DeLano Scientific LLC, San Carlos, CA (www.pymol.org).
20. Martin, J. L., and McMillan, F. M. (2002) SAM (dependent) I AM: the S-adenosylmethionine-dependent methyltransferase fold. *Curr. Opin. Struct. Biol. 12*, 783–793.
21. Schubert, H. L., Blumenthal, R. M., and Cheng, X. (2003) Many paths to methyltransfer: a chronicle of convergence. *Trends Biochem. Sci. 28*, 329–335.
22. Kozbial, P. Z., and Mushegian, A. R. (2005) Natural history of S-adenosylmethionine-binding proteins. *BMC Struct. Biol. 5*, 19.
23. Holm, L., and Sander, C. (1993) Protein structure comparison by alignment of distance matrices. *J. Mol. Biol. 233*, 123–138.

24. Martin, J. L., Begun, J., McLeish, M. J., Caine, J. M., and Grunewald, G. L. (2001) Getting the adrenaline going: crystal structure of the adrenaline-synthesizing enzyme PNMT. *Structure 9*, 977–985.
25. Horton, J. R., Sawada, K., Nishibori, M., and Cheng, X. (2005) Structural basis for inhibition of histamine N-methyltransferase by diverse drugs. *J. Mol. Biol. 353*, 334–344.
26. Zubieta, C., Ross, J. R., Koscheski, P., Yang, Y., Pichersky, E., and Noel, J. P. (2003) Structural basis for substrate recognition in the salicylic acid carboxyl methyltransferase family. *Plant Cell 15*, 1704–1716.
27. Schubert, H. L., Phillips, J. D., and Hill, C. P. (2003) Structures along the catalytic pathway of PrmC/HemK, an N5-glutamine AdoMet-dependent methyltransferase. *Biochemistry 42*, 5592–5599.
28. Korolev, S., Ikeguchi, Y., Skarina, T., Beasley, S., Arrowsmith, C., Edwards, A., Joachimiak, A., Pegg, A. E., and Savchenko, A. (2002) The crystal structure of spermidine synthase with a multisubstrate adduct inhibitor. *Nat. Struct. Biol. 9*, 27–31.
29. Lim, K., Zhang, H., Tempczyk, A., Bonander, N., Toedt, J., Howard, A., Eisenstein, E., and Herzberg, O. (2001) Crystal structure of YecO from *Haemophilus influenzae* (HI0319) reveals a methyltransferase fold and a bound S-adenosylhomocysteine. *Proteins 45*, 397–407.
30. Krynetski, E. Y., Krynetskaia, N. F., Yanishevski, Y., and Evans, W. E. (1995) Methylation of mercaptopurine, thioguanine, and their nucleotide metabolites by heterologously expressed human thiopurine S-methyltransferase. *Mol. Pharmacol. 47*, 1141–1147.
31. Woodard, R. W., Tsai, M. D., Floss, H. G., Crooks, P. A., and Coward, J. K. (1980) Stereochemical course of the transmethylation catalyzed by catechol O-methyltransferase. *J. Biol. Chem. 255*, 9124–9127.
32. Woodson, L. C., Ames, M. M., Selassie, C. D., Hansch, C., and Weinshilboum, R. M. (1983) Thiopurine methyltransferase. Aromatic thiol substrates and inhibition by benzoic acid derivatives. *Mol. Pharmacol. 24*, 471–478.
33. Ames, M. M., Selassie, C. D., Woodson, L. C., Van Loon, J. A., Hansch, C., and Weinshilboum, R. M. (1986) Thiopurine methyltransferase: structure-activity relationships for benzoic acid inhibitors and thiophenol substrates. *J. Med. Chem. 29*, 354–358.

BI800102X